Progress In Electromagnetics Research, Vol. 107, 101–114, 2010

DESIGN OF A HIGH BAND ISOLATION DIPLEXER FOR GPS AND WLAN SYSTEM USING MODIFIED STEPPED-IMPEDANCE RESONATORS

R.-Y. Yang

Department of Materials Engineering
National Ping-Tung University of Science and Technology
No. 1, Syuefu Rd., Neipu Township, Pingtung County 91201, Taiwan

C.-M. Hsiung

Department of Mechanical Engineering
National Ping-Tung University of Science and Technology
No. 1, Syuefu Rd., Neipu Township, Pingtung County 91207, Taiwan

C.-Y. Hung

Department of Electronics Engineering and Computer Sciences
Tung-Fang Institute of Technology
No. 110, Tung-Fung Road, Hunei Shiang
Kaohsiung County 829, Taiwan

C.-C. Lin

Department of Mechanical Engineering
National Ping-Tung University of Science and Technology
No. 1, Syuefu Rd., Neipu Township
Pingtung County 91207, Taiwan

Abstract—In this paper, we presented the design of a high performance diplexer for applications of global positioning system (GPS) at 1.575 GHz and wireless local area network (WLAN) at 2.4 GHz, simultaneously. Two bandpass filters (BPFs) using the modified stepped-impedance resonators (SIRs) operated at 1.575 GHz and 2.4 GHz are the main blocks for the proposed diplexer. By discussing and analyzing the admittance of the even and odd modes, the transmission zero of the modified SIR can be found, and the

Received 9 June 2010, Accepted 23 July 2010, Scheduled 2 August 2010
Corresponding author: C.-Y. Hung (goliro.goliro@msa.hinet.net).

location of the transmission zero can be precisely predicted, thus having a wide and deep stopband for the BPFs, useful for the high performance diplexer. Furthermore, due to the appearance of the transmission zeros near the passband edges, the passband selectivity of the BPFs as well as the diplexer can be improved. By using the impedance matching between two BPFs, a high isolation of 5 dB between two channels is obtained. The proposed diplexer was designed, fabricated and measured. The simulated and measured results had a good agreement with the proposed design concept.

1. INTRODUCTION

Recently, multi-service systems combined with Global Position System (GPS) at 1.575 GHz and the newly developed Wireless Local Area Network (WLAN) at IEEE 802.11b/g (2.4/2.45 GHz) are the most popular systems in the modern communications [1–4]. Diplexers are three terminal devices, letting two or more frequencies into one input port and then separating them to two other output ports. For such multi-service functions of the modern communication systems, compactsize and high performance planar diplexers are widely popular. In the past, some methods were reported to design diplexers [5–12]. For example, the ridge waveguide T-junctions were used for wideband diplexer applications [5, 6]. However, such waveguide configuration is hard to be integrated directly within a planar system. The most popular structures to form the planar diplexer are combing two bandpass filters (BPFs) with different frequencies and with two matching circuits, such as the balanced open-circuited periodic stubs [7,] and common resonators sections [8] are usually used. However, they increase the insertion loss and circuit size. In addition, two hairpin line filtering structures were used to form a diplexer, and a tapped open stub was used to introduce an attenuation pole to suppress the spurious response and achieve a high isolation between two bands [9]. Parallel coupled lines [10] square ring resonators [11] and dual-mode stepped-impedance resonator (SIR) [12] were also developed for the diplexer. However, the band isolation and upper stopband were still poor. In order to achieve the high band isolation and a wide stopband simultaneously, the above mentioned diplexers in fact have some problematic issues, such as large dimension or high insertion loss. In a previous work [13], a microstrip BPF using the modified SIR was designed and implemented, showing a wide and deep stopband. It is then expected that such BPF can be used for the high band isolation diplexer.

In this paper, we proposed a good band isolation diplexer used for the multi-service systems, such as the GPS at 1.575 GHz and WLAN at 2.4 GHz. In the first step, two square open-ring SIRs are modified and analysed to realize miniaturized BPFs to satisfy the required passbands. Additionally, by analyzing the admittance of the even and odd mode of the proposed SIR, the precise prediction of the location of the transmission zeros can be obtained to realize a high performance BPF with a wide and deep stopband as well as a sharp transition band. In the second step, two BPFs used for GPS at 1.575 GHz and WLAN at 2.4 GHz are designed to achieve the desired performances for the diplexer. In the third step, the two BPFs are combined. Due to the good impedance matching in input port for two BPFs, a high isolation between two channels is also obtained. In the forth step, the proposed diplexer is designed, fabricated and measured. The measured results of the fabricated diplexer have a good agreement with the simulated ones.

2. DESIGN PROCEDURE

Figure 1 is the geometry structure of the proposed diplexer. The BPFs in the proposed diplexer are two square open-ring BPFs using modified SIRs. The right part is the BPF section for GPS application, and the left part is the BPF section for WLAN application. In this paper, the diplexer, BPFs and SIRs are all designed on Duroid 5880 substrate with a thickness of 0.787 mm, dielectric constant ε_r of 2.2, and loss tangent of 0.0009. The input line with branch structure is tapped to two BPFs to provide the input power and impedance matching.

2.1. Analysis of the Modified SIR

In the first step, two square open-ring SIRs are modified and analysed to realize miniaturized BPFs to satisfy the required passbands for GPS at 1.575 GHz and WLAN at 2.4 GHz. Fig. 2 shows the structure of the conventional SIR and the proposed modified SIR by folding the conventional SIR to be the square open-loop SIR. The requirements of the BPFs for the diplexer are that first BPF with low center frequency shall have a wide upper stopband without interference with the frequency response of the second BPF, and the second BPF with high center frequency shall have a wide lower stopband without interference with the frequency response of the first BPF [11, 12]. Therefore, the resonator in the building block of the BPF shall also satisfy the condition. Generally, the former is more important since most of the resonators have the spurious responses, causing a poor

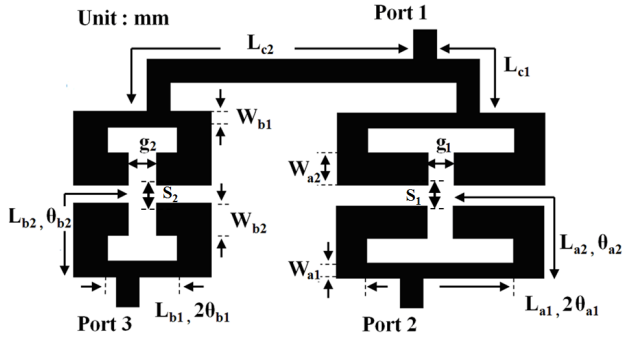

Figure 1. Schematic of the proposed diplexer. The right part is the BPF section for GPS application and the left part is the BPF section for WLAN application. The input line with branch structure is tapped to two BPFs provide the input power and the impedance matching.

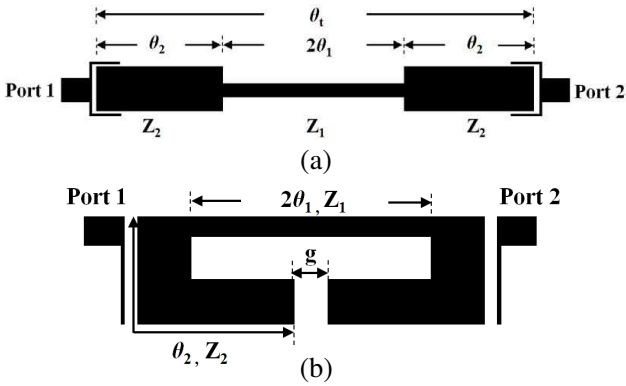

Figure 2. The structures of (a) the conventional SIR and (b) the modified SIR by folding the conventional SIR to be the square open-loop SIR.

stopband.

The following discusses the analysis of the modified SIR and design guide to obtain the desired center frequency. It is well-known that the SIR is formed by a high-impedance section ($Z_1 = 1/Y_1$) with an electrical length θ_1 and two low-impedance sections ($Z_2 = 1/Y_2$), each having an electrical length θ_2. The impedance ratio (R) of the SIR is defined as $R = Z_2/Z_1$, and the total electrical length of the conventional SIR is defined as θ_t. The resonance conditions of the

SIRs can be determined by one of the following equations [14]:

$$R \cdot \cot\theta_2 = \tan\theta_1 \tag{1}$$

$$R \cdot \cot\theta_2 = -\cot\theta_1 \tag{2}$$

Solutions regarding to (1) and (2) are the odd- and even-mode resonances, respectively. For more design freedoms, we adjusted the impedance ratio and electrical length of SIRs to achieve the fundamental resonances and the second resonances over a wide frequency range. Thus, the θ_2 is set as the variance, proportional to the electrical length of SIR, and the length ratio α of the SIR is defined as [14]

$$\alpha = \frac{\theta_2}{\theta_1 + \theta_2} = \frac{2\theta_2}{\theta_t} \tag{3}$$

After substituting (3) into (1) and (2), there are two designed parameters, the impedance ratio (R) and the length ratio (α) of the conventional SIR varied to adjust the higher order resonant modes nearly or far away the fundamental mode. When substituting Eq. (3) into Eqs. (1) and (2), there are many resonant possibilities corresponding to different R and α. Therefore, it is possible to achieve a broad stop band by properly selecting R and α, thus satisfying the requirement for the BPFs of the diplexer. In this paper, R of 0.53 and α of 0.69 are selected for the first SIR for 1.575 GHz, and R of 0.53 and α of 0.78 are selected for the second SIR for 2.4 GHz. Namely, the high-impedance ($Z_1 = 54\,\Omega$) line section with a physical length of 17.63 mm and the low-impedance ($Z_2 = 28.6\,\Omega$) line sections with a physical length width of 18.93 mm are set for the first SIR for 1.575 GHz, and the high-impedance ($Z_1 = 54\,\Omega$) line section with a physical length of 8.24 mm and the low-impedance ($Z_2 = 28.6\,\Omega$) line sections with a physical length width of 14.23 mm are set for the first SIR for 2.4 GHz.

Figure 3 is the simulated frequency response of the conventional SIR and the proposed square open-loop SIR for the center frequency at 1.575 GHz. It is clearly found that the frequency responses for the conventional SIR and the proposed square open-loop SIR are different. For the center frequency of $f_0 = 1.575$ GHz, the first spurious response f_1 of the conventional SIR is shifted to 4.2 GHz ($2.7f_0$), while the first spurious response f_1 of the proposed modified SIR can be shifted to 4.51 GHz ($2.9f_0$). Moreover, it is also found that the modified SIR as shown in Fig. 3 has a wide and deep stopband due to the existence of a transmission zero, indicating that the modified SIR not only further reduce the circuit size but also improve the stopband, compared to the conventional SIR. In order to precisely predict the location of the transmission zero, the analysis of the even and odd modes of the proposed SIR is used since the resonator is symmetric. The detailed

method to precisely predict the location of the transmission zero of the modified SIR was reported in a previous work and only simply addressed here [13]. The equivalent circuit of the even and odd modes for the proposed SIR is shown in Fig. 4. Y_{in}^{e} and Y_{in}^{o} are the input admittances of the even and odd modes, as shown in Fig. 4(a) and Fig. 4(b), respectively. Although the gap is usually equivalent to the shunt capacitance C_{12}, it was found that the gap g of the proposed SIR can be also modeled as equivalent length of transmission line Δl but not as the shunt capacitance C_{12}, as discussed in [13]. The corresponding resonant frequencies of the even and odd modes can be derived from (4) and (5), when $Y_{in}^{e} = 0$ or $Y_{in}^{o} = 0$ [15].

$$Y_{in}^{e} = j\left(\frac{\tan\theta_2}{Z_2} + \frac{\tan\theta_1}{Z_1}\right) \tag{4}$$

$$Y_{in}^{o} = -j\left(\frac{1}{Z_2\tan\theta_2} + \frac{1}{Z_1\tan\theta_1}\right) \tag{5}$$

Figure 4(b) shows the simulated result of the fundamental and first higher order resonant frequencies of the modified SIR at 1.575 GHz. Proper choice of the above parameters leads to an optimal reduction of circuit dimension and extension of upper rejection bandwidth. The $Z_1 = 54\,\Omega$, $Z_2 = 28.6\,\Omega$, $\theta_{a1} = 22.76^\circ$, $\theta_{a2} = 5.2^\circ$ are set for the calculated values of the Y_{in}^{e} and Y_{in}^{o}. It is seen that the fundamental resonance occurrs in the odd mode, and the first order resonance occurrs in the even mode. In addition, the locations of the transmission zero are precisely located as $Y_{in}^{o} = Y_{in}^{e}$. Therefore, it is believed that the modified SIR is very suitable to be used in the first BPF of the diplexer having a wide and deep stopband without interference with the frequency response of the second BPF.

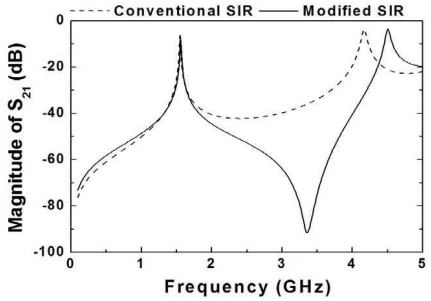

Figure 3. The simulated frequency responses of the conventional SIR and the modified SIR for 1.575 GHz.

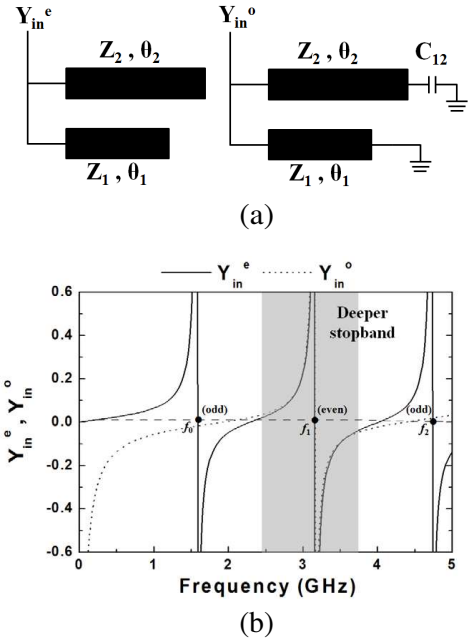

Figure 4. (a) Equivalent circuit for analysing even mode (Y_{in}^{e}) and odd mode (Y_{in}^{o}) of the modified SIR and (b) the calculated values of Y_{in}^{e} and Y_{in}^{o} as $Z_1 = 54\,\Omega$, $Z_2 = 28.6\,\Omega$, $L_{a1} = 17.63\,\text{mm}$, $L_{a2} = 18.93\,\text{mm}$ for 1.575 GHz.

2.2. Filter Design

In the second step, two BPFs used for GPS at 1.575 GHz and WLAN at 2.4 GHz are designed to achieve the desired performances for the diplexer. The 3-dB fractional bandwidth (FBW) at 1.575 GHz is set as FBW = 4.4% with the passband ripple of 1 dB. According to the desired target values, the lumped circuit element values of the Chebyshev low-pass prototype filter are found to be $g_1 = 1.8219$, and $g_2 = 0.6850$. On the other hand, the 3-dB FBW at 2.4 GHz is set as FBW = 3.5% with the passband ripple of 0.5 dB, thus the lumped circuit element values of the low-pass prototype filter are found to be $g_1 = 1.4029$ and $g_2 = 0.7071$. After knowing the lumped circuit element values, the desired coupling coefficient can be obtained as 0.0408 and 0.0345 for 1.575 GHz and 2.4 GHz respectively based on the classical coupling theory as $K = FBW/\sqrt{g_1 g_2}$ [15]. After selecting the impedance ratio ($R = Z_2//Z_1 = 0.53$) and length ratio α of 0.69 for 1.575 GHz and the impedance ratio ($R = Z_2//Z_1 = 0.53$) and length

ratio α of 0.78 for 2.4 GHz, two BPF prototypes are obtained. In this work, the spacing $S_1(S_2)$ between the modified SIRs is used to adjust the coupling coefficient to achieve the desired filter responses. The calculated coupling coefficient K between the modified SIRs is specified by the two dominant and splitting resonant frequencies due to the electromagnetic coupling. Coupling coefficient K is determined as [15]

$$K = \frac{f_{p2}^2 - f_{p1}^2}{f_{p2}^2 + f_{p1}^2} \tag{6}$$

where f_{p2} and f_{p1} are the higher and lower one of the two resonant frequencies, respectively. The coupling coefficients K shown in Fig. 5 are calculated by a full-wave EM simulator [16]. As shown, the coupling coefficient K decreases as the spacing $S_1(S_2)$ increases. When the spacing of $S_1(S_2)$ is small (0.2 mm), the stronger coupling leads to mode splitting. On the other hand, the larger spacing (0.7 mm) $S_1(S_2)$ make proper coupling. By mapping the required coupling coefficient into Fig. 5, the satisfactory spacing $S_1(S_2)$ is obtained. The filter performance is further simulated by using the EM simulator with slightly structural tuning [16]. After using the optimized structural parameters, two satisfactory performances of the BPFs using the modified SIRs as the fundamental building blocks are obtained. Fig. 6 is the simulated frequency responses of the designed BPFs for GPS and WLAN without the matching network. The first BPF operated at 1.575 GHz has a FBW of 4.4% and a spurious suppression more than 20 dB up to 4.4 GHz. Moreover, the first BPF has two transmission zeros located at 1.39 GHz and 1.84 GHz, with attenuation of 62 dB and 60 dB, respectively, much improving the band selectivity. The second BPF operated at 2.4 GHz has a FBW of 3.5% and a spurious suppression more than 30 dB up to 5 GHz. Similarly, the second BPF

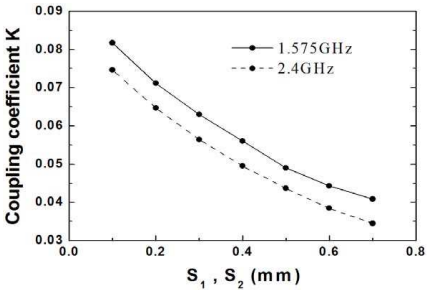

Figure 5. Coupling coefficients of the modified SIR for both of two BPFs.

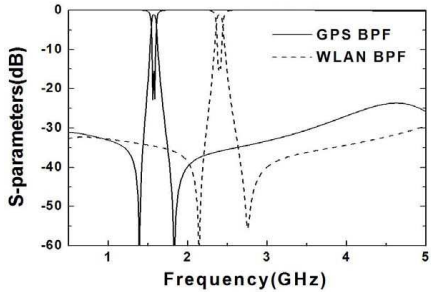

Figure 6. Simulated frequency responses of the designed BPFs for GPS and WLAN individually.

also has two transmission zeros located at 2.2 GHz and 2.7 GHz, with attenuation of 61.5 dB and 56.3 dB, respectively, which are expected to improve the band isolation.

(The structural parameters as defined in Fig. 1 are: $L_{a1} = 18.93\,\text{mm}$, $L_{a2} = 17.63\,\text{mm}$, $L_{b1} = 14.23\,\text{mm}$, $L_{b2} = 8.24\,\text{mm}$, $W_{a1} = 2.15\,\text{mm}$, $W_{a2} = 5.2\,\text{mm}$, $W_{b1} = 2.15\,\text{mm}$, $W_{b2} = 5.2\,\text{mm}$, $g_1 = 3.2\,\text{mm}$, $g_2 = 3.2\,\text{mm}$, $S_1 = 0.7\,\text{mm}$, $S_2 = 0.7\,\text{mm}$.)

2.3. Diplexer Design with the Impedance Matching

In the third step, the two BPFs are combined. It is known that although the filter performance of the individual BPF satisfies the required communication systems for the GPS and WLAN, the diplexer performance of the diplexer might be distorted after combing the two individual BPFs. As shown in Fig. 1, the common input port is

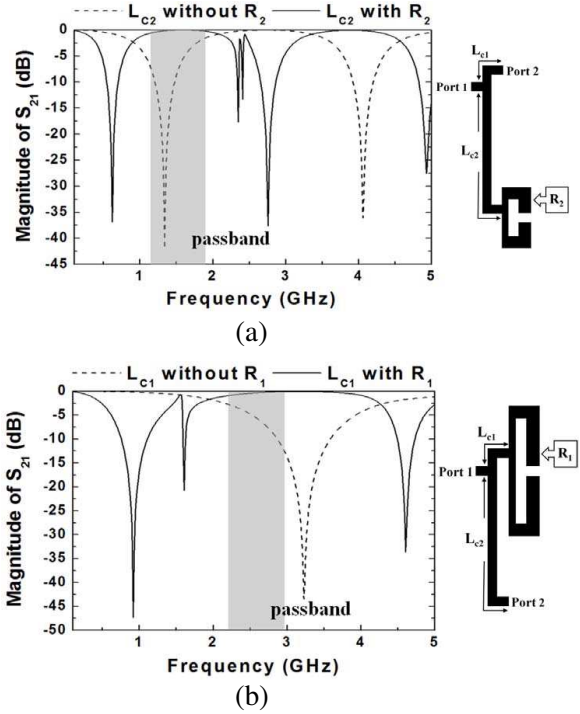

Figure 7. The simulated frequency responses of the tapped branch-structure coupling line as the matching load for (a) 1.575 GHz and (b) 2.4 GHz square open-ring BPFs.

port 1, and the output ports for the first and second BPFs are ports 2 and 3, respectively. The optimum coupling line length of the tapped branch-structure is designed to achieve the impedance matching of the diplexer. In this study, the lengths of the coupling lines (L_{c1} and L_{c2}) of the tapped branch structure are tuned for impedance matching. The required conditions of the impedance matching of the diplexer are set as: the input impedance seen into the second BPF is infinite when the first BPF is operated, and the input impedance seen into the first BPF is infinite when the second BPF is operated [7–11]. By the full-wave EM analysis, the stub lengths $L_{c1} = 10.9\,\text{mm}$ and $L_{c2} = 39.5\,\text{mm}$ are obtained for good impedance matching. Fig. 7 shows the simulated frequency responses of the tapped branch structure without and with different loads. As shown in Fig. 7(a), with the second BPF as the load, the first passband at 1.575 GHz is not affected, but the second passband at 2.4 GHz is suppressed. Similarly, as shown in Fig. 7(b),

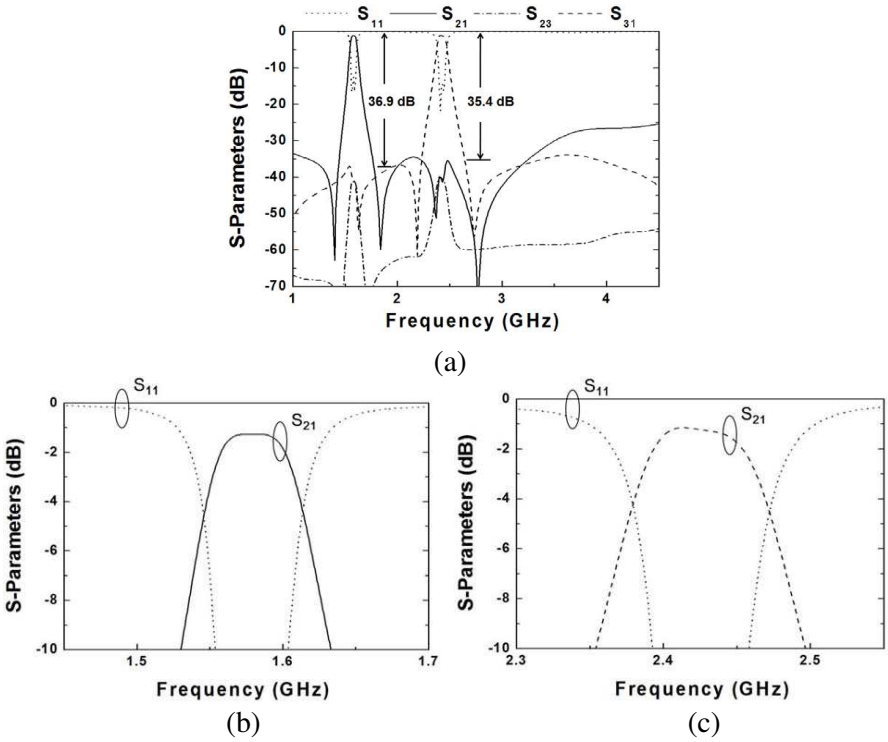

Figure 8. (a) Simulated frequency responses of the proposed diplexer with the impedance matching, and the simulated passbands at (b) 1.575 GHz and (c) 2.43 GHz in detail.

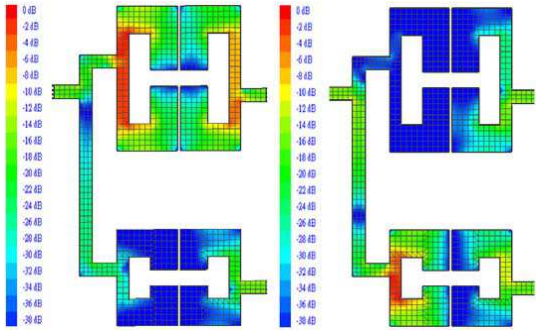

Figure 9. Simulated current distribution and coupling paths oscillating of the diplexer at the centre frequency at (a) 1.575 GHz and (b) 2.4 GHz.

with the first BPF as the load, the second passband at 2.4 GHz is not affected, but the first passband at 1.575 GHz is suppressed.

The simulated result of the diplexer by combining the two BPFs with matching network is shown in Fig. 8. And the simulated passbands at 1.575 GHz and 2.43 GHz are shown in detail in Fig. (b) and (c), respectively. Several transmission zeros still exist near the two passband edges in the designed diplexer, as appearing in two individual BPF shown in Fig. 6. Because the inter-rejection performance with the rejection level larger than 36.9 dB is pretty good, no passband is interfered. Moreover, a high isolation $|S_{23}|$ greater than 60 dB between two channels is obtained due to good impedance matching.

Figures 9(a) and (b) show the simulation current distribution for the diplexer operated at 1.575 and 2.4 GHz. The current distribution gives direct insight to understand the direction of the coupling paths and thus to easily make optimum design of the proposed diplexer structure. When operating at 1.575 GHz more current distribution is located on the first BPF since the input impedance seen into the second BPF is infinite, and the path to the second BPF is open. Similarly, when operating at 2.4 GHz more current distribution is located on the second BPF since the input impedance seen into the first BPF is infinite, and the path to the first BPF is open.

3. EXPERIMENTAL RESULTS AND DISCUSSION

In the forth step, the proposed diplexer was fabricated and measured by an HP8510C Network Analyser. Fig. 10(a) is the photograph of the fabricated diplexer. The fabricated diplexer has a small size, around 62 mm $\times$ 32 mm, i.e., approximately by $0.44\lambda_g \times 0.23\lambda_g$, where λ_g

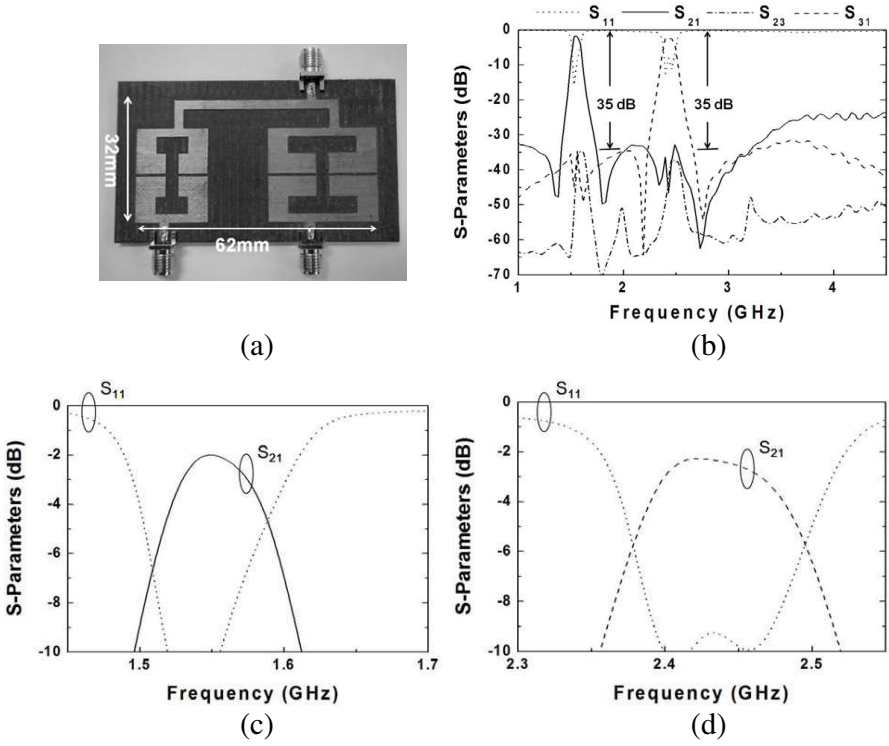

Figure 10. (a) Photograph and (b) measured frequency responses of the fabricated diplexer and the measured passbands at (c) 1.575 GHz and (d) 2.43 GHz in detail.

is the guided wavelength at the centre frequency at 1.575 GHz, or approximately by $0.67\lambda_g \times 0.35\lambda_g$, where λ_g is the guided wavelength at the centre frequency at 2.4 GHz. Fig. 10(b) is the measured results. The measured results for the first passband in diplexer include a centre frequency at 1.575 GHz with $|S_{21}|$ of 1.8 dB, a lower stopband rejection greater than 30 dB beyond 1.48 GHz and a higher stopband rejection greater than 25 dB from 1.67 to 4.5 GHz. The measured results for the second passband in diplexer include a centre frequency at 2.43 GHz with $|S_{31}|$ of 2.3 dB, a lower stopband rejection greater than 35 dB beyond 2.32 GHz and a higher stopband rejection greater than 30 dB from 2.58 to 4.5 GHz. Figs. 10(c) and (d) are the measured passbands at 1.575 GHz and 2.4 GHz in detail, respectively. Since we have made the matching network for the proposed diplexer, the insertion losses of the two passbands are mainly due to copper metalisation loss and the dielectric loss of the lossy substrate. By using the BPF with a

wide stopband, the inter-rejection level larger than 35 dB is obtained, and no passband is interfered. In addition, because of good impedance matching, the isolation between the two channels $|S_{23}|$ is better than 35 dB. Taking advantages of its simple design, compact size, and easy fabrication, the proposed diplexer actually has a good potential for the GPS and WLAN multi-service communication systems.

4. CONCLUSION

In this paper, we have presented the design of a high performance diplexer for GPS at 1.575 GHz and WLAN at 2.4 GHz. Two BPFs using modified SIRs are used as main structures to form the proposed diplexer since they can have a wide stopband and two transmission zeros near the passband edges to improve the passband selectivity and band isolation. The design procedures for the proposed diplexer are clearly discussed. The proposed diplexer was fabricated and measured to verify the design concept. The measured results for both the first and second passbands in diplexer satisfied the desired requirements. Moreover, the isolation $|S_{23}|$ better than 35 dB has been obtained due to good impedance matching. Measured results of the fabricated diplexer had a good agreement with the simulated ones.

REFERENCES

1. Xiong, J. P., L. Liu, X. M. Wang, J. Chen, and Y. L. Zhao, "Dual-band printed bent slots antenna for WLAN applications," *Journal of Electromagnetic Waves and Applications*, Vol. 22, No. 11–12, 1509–1515, 2008.
2. Hu, X., Q. Zhang, and S. He, "Compact dual-band rejection filter based on complementary meander line split ring resonator," *Progress In Electromagnetics Research Letters*, Vol. 8, 181–190, 2009.
3. Lee, C. H., I. C. Wang, and C. I. G. Hsu, "Dual-band balanced BPF using $\lambda/4$ stepped-impedance resonators and folded feed lines," *Journal of Electromagnetic Waves and Applications*, Vol. 23, No. 17–18, 2441–2449, 2009.
4. Ren, W., "Compact dual-band slot antenna for 2.4/5 GHz WLAN applications," *Progress In Electromagnetics Research B*, Vol. 8, 319–327, 2008.
5. Yao, W. H., A. E. Abdelmonem, J. F. Liang, X. P. Liang, K. A. Zaki, and A. Martin, "Wide-band waveguide and ridge

waveguide T-junctions for diplexer applications," *IEEE Trans. Microw. Theory Tech.*, Vol. 41, 2166–2173, 1993.

6. Han, S., X.-L. Wang, Y. Fan, Z. Yang, and Z. He, "The generalized Chebyshev substrate integrated waveguide diplexer," *Progress In Electromagnetics Research*, Vol. 73, 29–38, 2007.
7. Strassner, B. and K. Chang, "Wide-band low-loss high-isolation microstrip periodic-stub diplexer for multiple-frequency applications," *IEEE Trans. Microw. Theory Tech.*, Vol. 49, 1818–1820, 2001.
8. Chen, C. F., T. Y. Huang, C. P. Chou, and R. B. Wu, "Microstrip diplexers design with common resonator sections for compact size, but high isolation," *IEEE Trans. Microw. Theory Tech.*, Vol. 54, 1945–1952, 2006.
9. Deng, P. H., C. H. Wang, and C. H. Chen, "Compact microstrip diplexers based on a dual-passband filter," *Proceedings of Asia-Pacific Microwave Conference*, 2006.
10. Weng, M. H., C. Y. Hung, and Y. K. Su, "A hairpin line diplexer for direct sequence ultra-wideband wireless communications," *IEEE Microw. Wireless Compon. Lett.*, Vol. 17, 519–521, 2007.
11. Ye, C. S., Y. K. Su, M. H. Weng, and C. Y. Hung, "A microstrip ring-like diplexer for bluetooth and ultra wide band (UWB) application," *Microwave & Opt. Tech. Lett.*, Vol. 51, 1518–1520, 2009.
12. Huang, C. Y., M. H. Weng, C. S. Ye, and Y. X. Xu, "A high band isolation and wide stopband diplexer using dual-mode stepped-impedance resonators," *Progress In Electromagnetics Research*, Vol. 100, 299–308, 2010.
13. Yang, R. Y., C. M. Hsiung, C. Y. Hung, and C. C. Lin, "A high performance bandpass filter with a wide and deep stopband by using square stepped impedance resonators," *Journal of Electromagnetic Waves and Applications*, Vol. 24, 1673–1683, 2010.
14. Weng, M. H., C. H. Kao, and Y. C. Chang, "A compact dual-band bandpass filter with high band selectivity using cross-coupled asymmetric SIRs for WLANs," *Journal of Electromagnetic Waves and Applications*, Vol. 24, No. 2, 161–168, 2010.
15. Hong, J. S. and M. J. Lancaster, *Microstrip Filters for RF/Microwave Application*, John Wiley and Sons, 2001.
16. IE3D Simulator, Zeland Software, Inc., 1997.